PHYSICAL REVIEW D VOLUME 22, NUMBER 11 1 DECEMBER 1980

Inelastic thresholds and dibaryon resonances

Bonnie J. Edwards and Gerald H. Thomas
High Energy Physics Division, Argonne National Laboratory, Argonne, Illinois 60439
(Received 26 June 1980)

A method of Basdevant and Berger is applied to the problem of whether there are pp resonances near the $n\Delta^{++}$ threshold. In particular, the $^1D_2$ partial wave of proton-proton elastic scattering is analyzed around this threshold. The method is expected to determine (in principle) whether the pp partial waves in which structure has been observed are resonant and, in this event, allow a reliable determination of the resonance parameters.

I. INTRODUCTION

Remarkable structure has been observed in polarized proton-proton scattering data at intermediate energies, near the inelastic threshold for Δ^{++} production.[1] This structure has been interpreted by many as evidence for dibaryon resonances.[2] Furthermore, recent phase-shift analyses of these data indicate resonancelike behavior in the $^1D_2$ and $^3F_3$ partial waves.[3,4] Because the $n\Delta^{++}$ channel gives a large cross section in this energy range, there can be reasonable doubt whether the partial-wave structure observed corresponds to a second-sheet pole, or reflects solely the opening of a strong inelastic channel.[5]

Indeed the problem of what happens in one channel when one passes a strong threshold in a second channel is an old problem in strong-interaction dynamics.[6] Studies of high-lying πN resonances in πN phase shifts must take proper account of the effects of the inelastic channels in order to accurately extract the resonance parameters.[7] A notable example of resonancelike structure not necessarily accompanied by a resonance pole is the elastic K^+p system which caused speculation of the existence of an exotic Z resonance.[8]

The problem of properly accounting for a strong threshold opening in a many-channel problem is itself part of a larger problem, that of describing an amplitude when it contains a large, known background component. For example, the behavior of the 3π system in $\pi N \to \pi\pi\pi N$ is dominated by the one-pion-exchange process $\pi N \to (\pi\pi)\pi N$ which induces a 1^+ resonancelike structure. In addition, there is the possibility of a true 1^+ resonance (A_1) superimposed on this background. A similar problem occurs in $KN \to K\pi\pi N$ with the $(K\pi\pi)$ system given by a background generated by pion exchange, and a true 1^+ resonance (Q). A practical method for handling this problem has been proposed and applied to Q and A_1 production by Basdevant and Berger in a series of papers.[9,10] We apply their approach to the problem of dibaryons.

Specifically, we examine the $^1D_2$ $pp \to pp$ partial-wave amplitude near the threshold of the $n\Delta^{++}$ channel. Our treatment of the $^1D_2$ system differs from the phenomenological analysis of the phase shifts by Hoshizaki[3] in that we seek to understand the large background terms which, in that analysis, were added by hand. To do this we explicitly introduce the inelastic channels, rather than parametrizing their effect by the inelasticity parameter. In this way we are able to discuss some of the analytic constraints. In a practical sense, however, we expect our results to be qualitatively similar to Hoshizaki's for those things he is able to calculate.

The problem of dibaryons on pp scattering has been addressed by many authors.[11] Some have taken a purely dynamical approach, trying to understand the $NN\pi$ system through the NN and $N\pi$ forces. Others have used two-body dynamics as a starting point for a phenomenological analysis—for example, in an N/D calculation, the form of the N matrix has often been motivated by the one-boson-exchange model. In this paper, we make no assumption about the origin of the dynamics but attempt to reconstruct the S matrix from phase-shift information, subject only to the constraints of unitarity and analyticity. We consider only two-body and quasi-two-body channels, although some features of three-body unitarity are incorporated.

In Sec. II we present the methodology of the analysis of the $^1D_2$ system. In Sec. III we carry out the analysis on the presently available data.

II. METHODOLOGY

A. Choice of channels

In this paper we investigate the $J^P=2^+$ dibaryon system, leaving to a later paper the $J^P=3^-$ systems. Since one is above the π production threshold, there are many channels which couple to the elastic $pp(^1D_2)$ channel. The exclusive single-π states are $d\pi^+$ and $NN\pi$. In the foreseeable future one does not expect to have reliable phase-shift analyses for the inelastic processes. Lacking strong empirical guides, we have selected for study only one inelastic channel, the quasi-two-body $n\Delta^{++}(^5S_2)$. We assume that $n\Delta^{++}$ dominates the three-body final state $pn\pi^+$ (Ref. 12) and neglect the higher waves $n\Delta^{++}(^5D_2, ^5G_2, ^3D_2)$ which are suppressed by centrifugal-barrier factors.[13] The three-body process $pp \to pp\pi^0$ has only about 20% the cross section of $pp \to pn\pi^+$, and is neglected here. The remaining channels which can couple are $\pi^+d(^3P_2, ^3F_2)$. The π^+d channel is important at the single-π production threshold, but is less important than $np\pi^+$ for $s \gtrsim 4.4$ GeV^2, the region of interest.[14] In this analysis we do not include this channel.

To put these assumptions in perspective, note that at $p_{\text{lab}} = 1.2$ GeV/c ($s = 4.62$ GeV^2), the total inelastic pp cross section is approximately 10 mb, of which 1.2 mb is $pp\pi^0$, 2.5 mb is π^+d, and 6.3 mb is $pn\pi^+$. These cross sections are good to about 20% since they are based on crude interpolations of the measured cross sections which are not available at many energies in the region of interest. Moreover, the total inelastic spin-singlet contribution has been estimated by Hollas[5] to be only about 5 mb. This is consistent with the phase-shift solutions[3,4] which predict an inelastic $^1D_2$ cross section of about 5 mb, and negligible inelastic cross sections for the other singlet states. If the exclusive inelastic singlet cross sections are in the same ratio as the total, then one would estimate the singlet $pp\pi^0$, π^+d, and $pn\pi^+$ cross sections as 0.6, 1.2, and 3.2 mb, respectively. These estimates are not unreasonable since the presence of substantial polarization[15] in $pp \to \pi^+d$ scattering indicates that the inelastic cross section for this process is shared among at least two partial waves, thus considerably reducing the π^+d contribution to $pp(^1D_2)$ inelastic scattering from 2.5 mb.

We conclude from this discussion that there are a variety of uncertainties in estimating the exclusive singlet cross sections which could easily amount to 1–2 mb in the $^1D_2$ cross section. We are searching for a resonance effect which, if Hoshizaki's background can be used as a guide, amounts to about 2 mb out of the 5-mb $^1D_2$ inelastic cross section at the resonance peak $s \cong 4.62$ GeV^2. This resonance effect is not much larger than what we estimate for the π^+d contribution, or the uncertainty in the inelastic $^1D_2$ cross section.[16] The restriction to the two channels $pp(^1D_2)$ and $n\Delta^{++}(^5S_2)$ should therefore be taken as provisional, and could be improved as more is learned about the partial-wave structure of the inelastic channels. In defense of this approximation, however, we note that none of the effects we ignore are expected to have a sharp energy dependence over the region we are discussing. Our analysis may suggest the extent to which the appearance of a resonance depends on the energy dependence of the partial-wave amplitude though not on its precise values.

B. K-matrix approximations

Our goal is to analytically continue the scattering matrix away from physical s and search for poles which would be indicative of dibaryon resonances. Since only the elastic component of the scattering matrix has been partial-wave analyzed, an inherent ambiguity is present in a multichannel program and only relatively simple parametrizations of the scattering matrix are warranted. The K-matrix formalism provides a way to construct an analytic unitary scattering matrix from phase shifts and also has the feature of admitting simple parametrizations.[17,18] To set the notation, we reproduce below some formalities.

Consider an N-channel problem in which the N-channel unitary $\mathcal{S}$ matrix has been exactly determined experimentally to all energies above the elastic threshold.[19] In this paper N is 2. For the moment we assume channel i consists of two stable particles with masses m_i and M_i in an orbital angular momentum state L_i. At a c.m. energy $\sqrt{s}$, the unitary symmetric $\mathcal{S}$ matrix, $\mathcal{S}(s)$, is related to the partial-wave $\mathcal{T}$ matrix by

$$\mathcal{S}(s) = 1 + 2i\mathcal{T}(s). \tag{2.1}$$

This $\mathcal{T}$ matrix contains threshold factors, which when removed define the boundary value of an analytic T matrix

$$T(s) = \rho(s)^{-1/2}\mathcal{T}(s)\rho(s)^{-1/2}, \tag{2.2}$$

where $\rho(s)$ is a diagonal matrix whose value in the ith channel is

$$\rho_i(s) = \left\{\frac{[s-(M_i+m_i)^2][s-(M_i-m_i)^2]}{s^2}\right\}^{(2L_i+1)/2}. \tag{2.3}$$

Corresponding to the T matrix is a nonunitary S matrix

$$\begin{aligned} S(s) &\equiv 1 + 2i\rho(s)T(s) \\ &= \rho^{1/2}(s)\mathcal{S}(s)\rho^{-1/2}(s). \end{aligned} \tag{2.4}$$

This S matrix satisfies $S^*S = SS^* = 1$ and will be useful in the discussion that follows.

The real analytic symmetric matrix $T(s)$ is defined in the complex s plane, is analytic in the upper half plane with left- and right-hand cuts along the real s axis. Across the right-hand cut

$$T(s^+) - T(s^-) = 2iT(s^+)\rho T(s^-) \tag{2.5}$$

and reproduces the unitarity condition $\mathcal{S}^+\mathcal{S} = I$. The K-matrix approximation to T is

$$T(s) = K(s)[1 - C(s)K(s)]^{-1}, \tag{2.6}$$

where $C(s)$ is the Chew-Mandelstam function satisfying

$$C(s^+) - C(s^-) = 2i\rho(s) \tag{2.7}$$

and K is a symmetric matrix whose elements are real analytic meromorphic functions of s. For K the unitarity condition is

$$1 - C(s^-)K(s) = S(s)[1 - C(s^+)K(s)]. \tag{2.8}$$

This shows that the K matrix provides a solution to the Hilbert problem.[20]

The Hilbert problem is that of finding a real analytic function $D(s)$ with only a right-hand cut whose boundary values satisfy

$$D(s^-) = S(s)D(s^+). \tag{2.9}$$

In general this problem is solved by finding an integral equation for $\mathrm{Im}D(s)$. Specifically, one defines $N(s)$ by

$$D(s^+) - D(s^-) = -2i\rho(s)N(s) \tag{2.10}$$

and writes a once subtracted dispersion relation for $D(s)$:

$$D(s^\pm) = 1 - \frac{s}{\pi}\int_{s_0}^{\infty} ds' \frac{\rho(s')N(s')}{s'(s'-s \mp i\epsilon)}. \tag{2.11}$$

Then, $N(s)$ satisfies the integral equation

$$N(s) = G(s)\left[1 - \frac{s}{\pi}P\int_{s_0}^{\infty} ds' \frac{\rho(s')N(s')}{s'(s'-s)}\right], \tag{2.12}$$

where the symmetric matrix $G(s)$ is defined by

$$G \equiv T(1 + i\rho T)^{-1}. \tag{2.13}$$

The integral equation involves quantities evaluated only in the physical region and therefore can be solved whenever the scattering matrix T is given.

The T matrix is given by

$$T(s) = N(s)D^{-1}(s)$$

so that when one continues T into the complex s plane one needs to continue both $N(s)$ and $D(s)$.

The solution to the Hilbert problem provides the analytic continuation of $D(s)$, but not $N(s)$. In general $N(s)$ will be real analytic with left-hand cuts.

The K-matrix approximation in essence replaces $N(s)$ by a meromorphic function. $K(s)$ is determined algebraically from the scattering data using (2.8):

$$K(s) = [S(s)C(s^+) - C(s^-)]^{-1}[S(s) - I] \tag{2.14}$$

rather than through the integral equation (2.12). As a solution to the Hilbert problem, $(1 - CK)$ is well determined for complex s.

C. Chew-Mandelstam functions

The parametrization (2.6) will be complete once the Chew-Mandelstam matrix $C(s)$ is defined, and the form for K is chosen. Now $(1 - CK)$ is like a D function which has an intrinsic polynomial ambiguity. We choose to put this ambiguity into K and use a canonical definition for C:

$$C(s) = \frac{s}{\pi}\int_{S_0}^{\infty} ds' \frac{\rho(s')}{s'(s'-s)} \tag{2.15}$$

The Chew-Mandelstam function for channel 1, pp elastic scattering in the ${}^1D_2$ state, may be obtained from (2.15) using

$$\rho_1(s, m_p, m_p) = \left(\frac{s - 4m_p^2}{s}\right)^{5/2}. \tag{2.16}$$

Near the pp elastic threshold,

$$\rho_1 \propto p_{1\mathrm{ab}}^5$$

as expected of an $L = 2$ wave. The total Chew-Mandelstam function is

$$C_1(s, m_p, m_p') = \frac{-2}{\pi}\left[\rho_1(s, m_p, m_p)\ln\frac{(4m_p^2 - s)^{1/2} + (-s)^{1/2}}{2m_p} - \left(\frac{4m_p^2}{s}\right)^2 + \frac{7}{3}\frac{4m_p^2}{s} - \frac{23}{15}\right]. \tag{2.17}$$

Note that C_1 is real for $s < 4m_p^2$, has a discontinuity of $2i\rho_1$ for $s > 4m_p^2$, and vanishes at $s = 0$.

The kinematics for channel 2, $n\Delta^{++}$ scattering in the ${}^5S_2$ state, are complicated by the instability of the Δ^{++} which decays predominantly into $p\pi^+$. If the Δ^{++} were stable, the Chew-Mandelstam function for $n\Delta^{++}$ would be that appropriate to two particles of unequal masses in an $L = 0$ state:

$$\rho_2(s, m_\Delta, m_n) = \frac{[s - (m_\Delta + m_n)^2]^{1/2}[s - (m_\Delta - m_n)^2]^{1/2}}{s}, \tag{2.18}$$

$$C_2(s, m_\Delta, m_n) = -\frac{2}{\pi}\left\{\rho_2(s, m_\Delta, m_n) \ln \frac{[(m_\Delta + m_n)^2 - s]^{1/2} + [(m_\Delta - m_n)^2 - s]^{1/2}}{2(m_\Delta m_n)^{1/2}}\right.$$
$$\left. + \frac{m_\Delta{}^2 - m_n{}^2}{2s} \ln\frac{m_\Delta}{m_n} - \frac{m_\Delta{}^2 + m_n{}^2}{2(m_\Delta{}^2 - m_n{}^2)} \ln\frac{m_\Delta}{m_n} - \frac{1}{2}\right\}. \quad (2.19)$$

C_2 is real below threshold, has a discontinuity of $2i\rho_2$ above threshold, and vanishes at $s = 0$.

Berger and Basdevant give a practical prescription for smearing this stable-particle Chew-Mandelstam function to obtain one with both a three-particle ($np\pi^+$) and a quasi-two-particle ($n\Delta^{++}$) cut.[10] They point out that the Chew-Mandelstam function arises from a loop integration in a simple Feynman graph and that the instability of one of the particles may be generated by the replacement of the usual stable-particle propagator by an unstable particle propagator:

$$\frac{1}{s - m_\Delta{}^2} \to \frac{1}{s - m^2 + f^2\Sigma(s)} = \frac{1}{d(s)}. \quad (2.20)$$

The parameters m and f are chosen so the propagator has a pole on the unphysical sheet at

$$s = (m_\Delta - i\Gamma_\Delta/2)^2 = m_\Delta^{*2}. \quad (2.21)$$

The full Chew-Mandelstam function is

$$C_2(s, m_\Delta^*, m_n) = \frac{1}{\pi}\int_{(m_p + m_\pi)^2}^{\infty} ds' \, \frac{f^2 \mathrm{Im}\Sigma(s')}{|s' - m^2 - f^2\Sigma(s')|^2} \times C_2(s, \sqrt{s'}, m_n). \quad (2.22)$$

This represents the smearing of the stable Chew-Mandelstam function over a range of Δ masses, the weighting function containing all relevant information concerning the Δ mass, width, and decay kinematics.

Following Berger and Basdevant's treatment of the ρ and K^* propagators, we approximate the self-energy part of $d(s)$ by

$$\Sigma(s) = [s - (m_p + m_\pi)^2] C^{L=0}(s, m_p, m_\pi), \quad (2.23)$$

where the $p\pi$ Chew-Mandelstam function has the same form as (2.19). This self-energy function has the proper threshold behavior for the decay of an $L = 1$ state. The validity of our approximation may be checked by examining the $p\pi^+$ phase shifts that $d(s)$ predicts. The $p\pi^+$ phases so predicted agree well with experiment[21] from threshold to above the Δ^{++} resonance ($1.16 < s < 1.63$ GeV^2; $0 < T_\pi < 0.25$ GeV); at higher energies, the predicted phases approach 180° but not so quickly as experiment suggests. It is interesting that, for physical s, the smeared Chew-Mandelstam function defined by (2.22) is numerically similar to that which would be obtained by using $m_\Delta^* = m_\Delta - i\Gamma_\Delta/2$ instead of m_Δ in the stable-particle function (2.19). As a result, the smeared Chew-Mandelstam function is insensitive to the subtleties of $d(s)$ away from $s = m_\Delta^{*2}$.

Throughout this analysis we use standard particle masses and widths[22]: $m_p = 938.3$ MeV, $m_n = 939.6$ MeV, $m_{\pi^+} = 139.57$ MeV, $m_\Delta^* = (1211 - i49.9)$ MeV. The resulting propagator parameters are $f^2 = 2.3217$ and $m^2 = 1.9252$ GeV^2. Of later interest is the derivative of the propagator evaluated at the Δ mass: $d'(m_\Delta^{*2}) = 2.0807 + i1.3242$.

D. Parametrization of K

The general form of the physical $\mathcal{S}$ matrix is

$$\mathcal{S} = \begin{pmatrix} \eta e^{2i\delta_1} & i(1-\eta^2)^{1/2} e^{i(\delta_1+\delta_2)} \\ i(1-\eta^2)^{1/2} e^{i(\delta_1+\delta_2)} & \eta e^{2i\delta_2} \end{pmatrix}, \quad (2.24)$$

where η is the inelasticity parameter and δ_1 and δ_2 are the phase shifts for channels 1 and 2, respectively. Recent phase-shift analyses by Arndt[4] and Hoshizaki[3] have determined η and δ_1 fairly consistently up to $s \simeq 5.1$ GeV^2 ($p_{\rm lab} \simeq 1.5$ GeV/c). At present, δ_2 is totally unconstrained, although conceivably polarization data now under analysis for $pp \to pn\pi^+$ will provide some crude $n\Delta^{++}$ constraints.[23]

The range and quality of the $pp(^1D_2)$ elastic data and the lack of $n\Delta^{++}$ phases introduces unavoidable ambiguities into the K matrix (2.14). Quite different K matrices which make consistent pp elastic scattering predictions may differ substantially in their prediction of δ_2 and, thereby, of $pp \to n\Delta^{++}$ inelastic scattering cross sections.

The energy range of interest is from $np\pi^+$ threshold ($s \simeq 4.1$ GeV^2) to the limits of the pp elastic phase shifts ($s \simeq 5.3$ GeV^2). For such a limited range of s, a variety of meromorphic K matrices may be expected to reproduce the measured η and δ_1 values. We chose to parametrize the K-matrix elements as simple polynomials:

$$K_{ij} = a_{ij} + b_{ij}s + c_{ij}s^2. \quad (2.25)$$

III. PHENOMENOLOGY

A. Fits

We present four solutions for K and their varying consequences. The parameters of these solutions are given in Table I and the phase and inelasticity predictions are shown in Figs. 1–4.

TABLE I. Summary of solutions.

	Solution 1	Solution 2	Solution 3	Solution 4
K_{11}: a_{11}	36.0	−147.1730	32.1700	−203.1460
b_{11} (GeV^{-2})	−6.0	68.1340	5.7	111.6128
c_{11} (GeV^{-4})	0.0	−7.8073	0.0	−15.0
K_{12}: a_{12}	2.8162	94.2323	−1.6798	217.7444
b_{12} (GeV^{-2})	0.0	−43.2066	1.5063	−106.5620
c_{12} (GeV^{-4})	0.0	5.0	−0.1761	13.1169
K_{22}: a_{22}	16.4081	−34.1870	21.8599	−135.2610
b_{22} (GeV^{-2})	−2.2947	21.5884	−4.9056	70.6292
c_{22} (GeV^{-4})	0.0	−2.9047	0.2777	−8.8764
Re(s_R) (GeV^2)	4.705	4.560	4.582	4.592
Im(s_R) (GeV^2)	−0.271	−0.232	−0.454	−0.231
M_R (GeV)	2.17	2.14	2.14	2.14
Γ (MeV)	125	108	212	108
Γ_1 (MeV	57	13	51	28
Γ_2 (MeV)	68	95	161	80

These solutions are representative of several dozen we obtained. Note that in the figures the solid curve is the result of our analysis. It is compared to the energy-dependent phase-shift solutions of Arndt[4] (dashed curve) and Hoshizaki[3] (crosses). No uncertainties are plotted for these phase-shift solutions, although a rough measure of their systematic error may be obtained by contrasting the two solutions. These systematic differences are typically larger than the statistical errors quoted[3,4] for the phase-shift fits.

Solution 1 (Fig. 1) illustrates all the important features of the analysis while using a very simple K matrix—K_{11} and K_{22} are linear in s, K_{12} is a constant. The $n\Delta^{++}$ phase rises slowly from threshold, peaks at about 10° at $s=4.7$ GeV^2, returns slowly through 0° at $s=5.0$ GeV^2. Solutions 2–4 use the full quadratic form of K and reproduce the pp elastic phases somewhat better. Solution 2 uses a K matrix with K_{11} and K_{12} small compared to K_{22} at threshold. This solution could be interpreted in a final-state interaction framework, with strong $n\Delta^{++}$ elastic scattering being reflected by unitarity in the pp channel. Consistent with this view is an $n\Delta^{++}$ phase which arises dramatically to about 50° at $s=4.7$ GeV^2. Solution 3 shows a quite different $n\Delta^{++}$ channel behavior—δ_2 remains essentially at 0° until $s=4.7$ GeV^2, whereupon it goes quickly negative. Solution 4 shows a δ_2 behavior not unlike that of solution 2, while demonstrating a larger variation in the K-matrix elements than any of the other solutions.

Common to all the solutions is a difficulty in obtaining an inelasticity which drops quickly enough just above $np\pi^+$ threshold. Since this is the energy region where the $pp\to\pi^+d$ cross section is largest, the inclusion of the π^+d inelastic channel might remedy this problem. For s near the upper limit of consideration, solutions 1 and 4 have pp phases which pass through 0°, while solutions 2 and 3 have pp phases which fall less sharply. These behaviors are similar to those of Hoshizaki's[3] and Arndt's[4] phase shifts, respectively. There is no correlation between the behavior of δ_1 at high s and the type of behavior of δ_2.

B. Resonance structure

We adopt as the definition of a resonance the occurrence of a pole in the $\mathcal{S}$ matrix at complex s near the physical region.[17,18] Equivalently, a resonance appears as a pole in the T matrix. Since our parametrization of the K matrix is well behaved, a pole occurs only when

$$\det(1-CK)=0. \tag{3.1}$$

The coupling strengths of a resonance to the various channels are determined by the residues

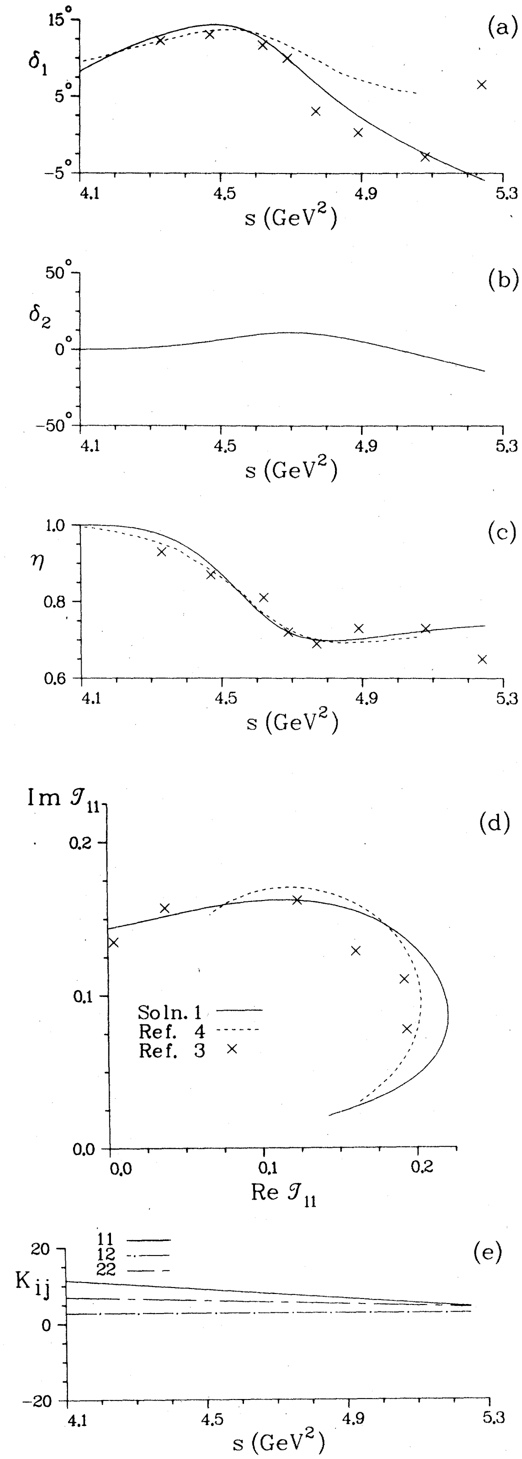

FIG. 1. Comparison of solution 1 (solid) with phase-shift analyses (dashed and crosses).

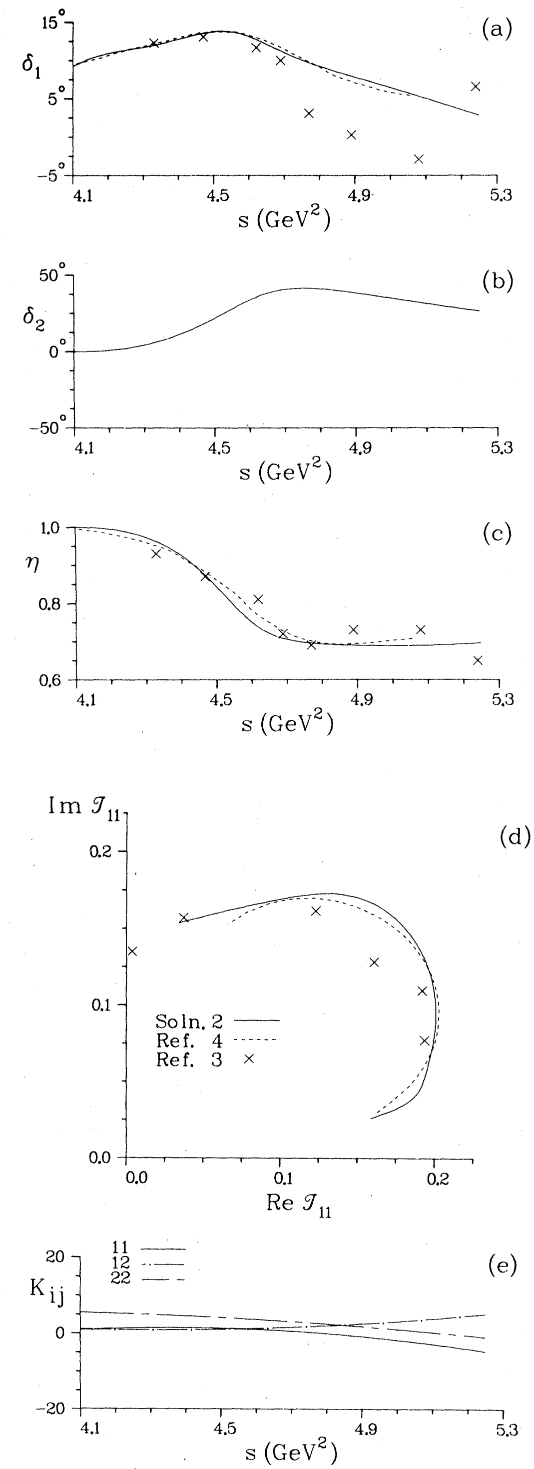

FIG. 2. Comparison of solution 2 (solid) with phase-shift analyses (dashed and crosses).

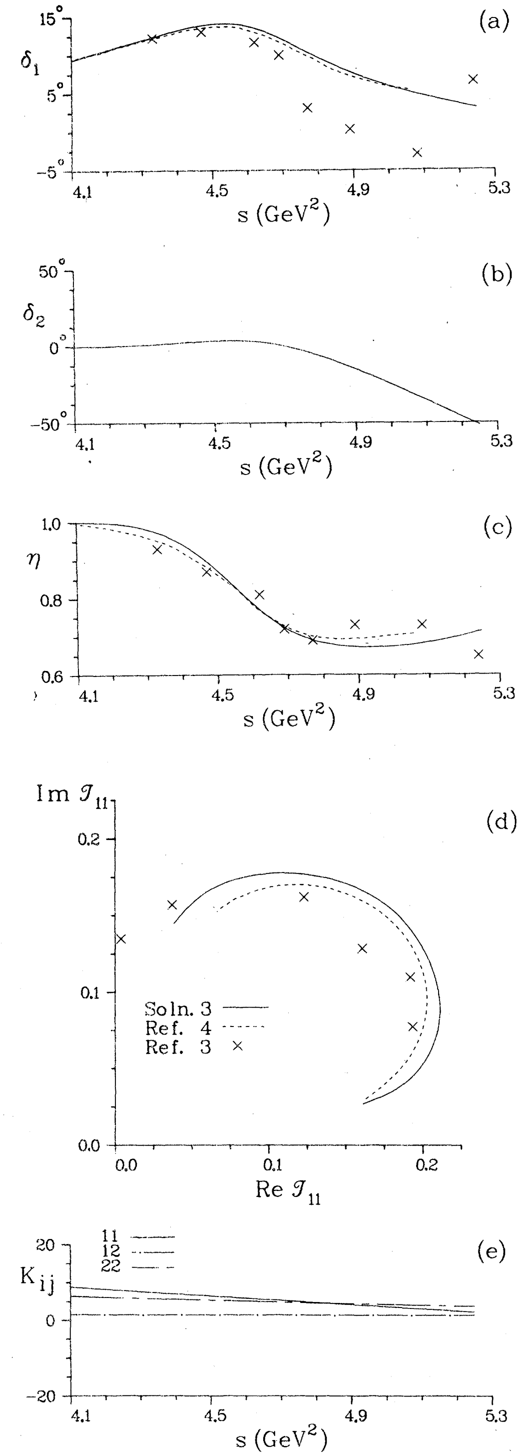

FIG. 3. Comparison of solution 3 (solid) with phase-shift analyses (dashed and crosses).

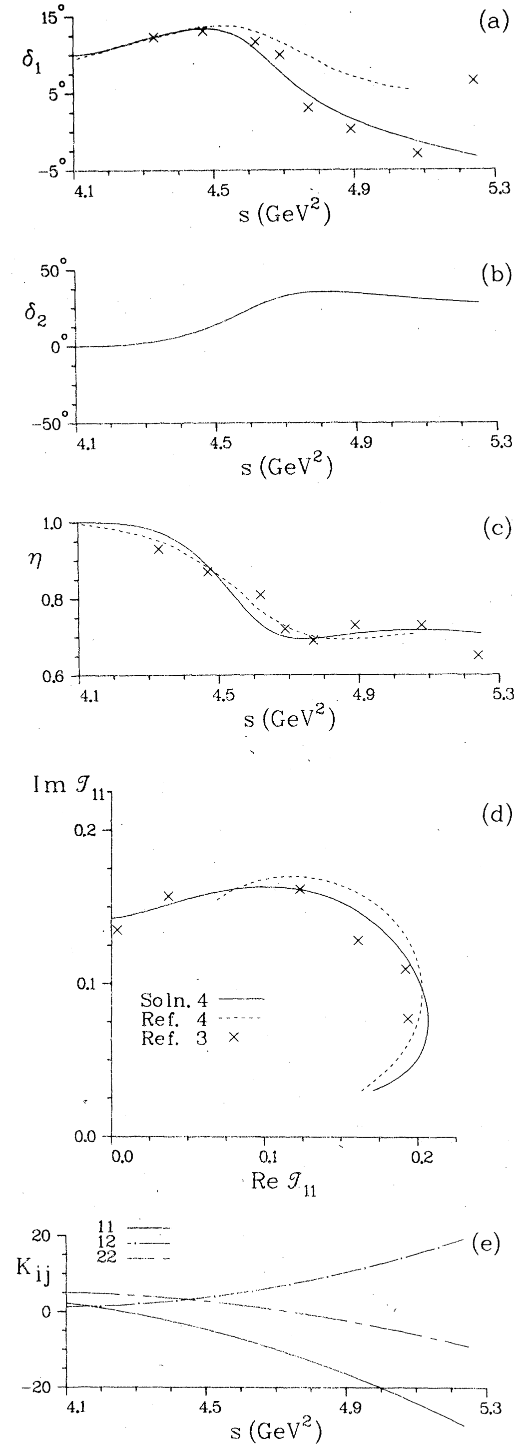

FIG. 4. Comparison of solution 4 (solid) with phase-shift analyses (dashed and crosses).

of the T matrix at the resonance pole. It is convenient to use the T matrix, rather than the $\mathcal{S}$ or $\mathcal{T}$ matrix, because the kinematical factors are automatically removed.[24] Near the resonance position s_R,

$$T_{ij} \sim -\frac{g_i g_j M_R}{s - s_R} e^{i(\phi_i + \phi_j)} + T_{ij}^0 , \tag{3.2}$$

where g_i is the coupling of the resonance to channel i and T_{ij}^0 is a well-behaved background contribution. The phases in the pole term arise from the background contribution in a way analogous to Watson's theorem. Since the K matrix or, equivalently, the N matrix is needed to determine the residues, the arguments of Sec. II suggest that the residues are subject to more uncertainty than the determination of the pole position.

The analytic continuation of K, C_1, and C_2 is needed to conduct a resonance search. The K matrix, being a polynomial in s, extends straightforwardly to complex s with no sheet structure. The Chew-Mandelstam functions are more complicated (see the Appendix), their cuts giving rise to many sheets. C_1, [Eq. (2.17)] has a pp cut from $4m_p^2$ to ∞ while C_2 [Eq. (2.22)] has an $np\pi^+$ cut from $(m_n+m_p+m_\pi)^2$ to ∞ and, on the second sheet of this cut, an $n\Delta^{++}$ cut from $(m_n+m_\Delta^*)^2$ to ∞. These cuts and the s regions of interest are illustrated in Fig. 5.

Region (i), the physical region, is on the first sheet of all the cuts (use $C_1^{\mathrm{I}}, C_2^{\mathrm{I}}$) and has Re$s \gtrsim 4m_p^2$, Im$s \gtrsim 0$. Region (ii) is reached by passing through the pp cut below $np\pi^+$ threshold [$4m_p^2 \lesssim$ Re$s \lesssim (m_n+m_p+m_\pi)^2$, Im$s \lesssim 0$] and is on the second sheet of the pp cut while on the first of the other two cuts (use $C_1^{\mathrm{II}}, C_2^{\mathrm{I}}$). Passing through both the pp and $np\pi$ cuts [Re$s \gtrsim (m_n+m_p+m_\pi)^2$, Im$s \lesssim 0$] region (iii) is found; it is on the second sheet of the pp and $np\pi^+$ cuts and on the first sheet of the $n\Delta^{++}$ cut (use $C_1^{\mathrm{II}}, C_2^{\mathrm{II}}$). Still further, through the $n\Delta^{++}$ cut, is region (iv) [Re$(s-(m_n+m_\Delta^*)^2) \gtrsim 0$, Im$(s-(m_n+m_\Delta^*)^2) \lesssim 0$]; this is on the second sheet of all the cuts (use $C_1^{\mathrm{II}}, C_2^{\mathrm{III}}$). A pole in regions (ii)–(iv) is interpreted as a resonance, a pole on the physical sheet on the real axis is a bound state or virtual bound state and any other pole on the physical sheet is a ghost (unphysical resonance). A resonance pole on (ii), (iii), or (iv) is expected to reoccur at a shifted position on one of the four sheets which are farther from the physical region and which have not been described. This fact provides an alternate method for extracting the resonance parameters.[25]

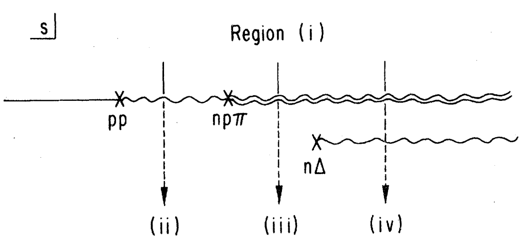

FIG. 5. The complex s plane. The pp, $np\pi^+$, and $n\Delta^{++}$ unitarity cuts are illustrated.

All of the solutions we obtained display a nearby pole in region (iii) (i.e., on second sheet of the pp and $np\pi^+$ cuts, on the first sheet of the $n\Delta^{++}$ cut) not far from the $n\Delta^{++}$ branch point. The pole positions and partial widths for solutions 1–4 are given in Table I. Two trends among the solutions are observed. Solutions whose δ_1 behavior resembles Hoshizaki's phase shifts[3] more closely than Arndt's[4] (δ_1 passes through 0° around $s = 5.0$ GeV^2) display poles close to the physical region—Γ as low as 70 MeV. Solutions whose δ_2 behavior resembles that of solution 3 (δ_2 remains near 0° until $s = 4.7$ GeV^2 and then goes sharply negative) exhibit quite distant poles and relatively large coupling to the pp channel—Γ as large as 220 MeV and Γ_1 as large as 60 MeV. Based on all the solutions we obtained we estimate

$$M_R = 2.14\text{–}2.16 \text{ GeV},$$

$$\Gamma = 70\text{–}220 \text{ MeV},$$

$$\Gamma_1 = 10\text{–}60 \text{ MeV},$$

$$\Gamma_2 = 60\text{–}160 \text{ MeV}.$$

These results are consistent with those of previous single-channel analyses.[3]

A search of regions (ii)–(iv) yields no further poles. On (i), in some solutions, a ghost is present (Re$s \lesssim 4.0$ GeV^2, Im$s \gtrsim 0.3$ GeV^2). Ghosts are symptomatic of the breakdown of an approximation in the $\mathcal{S}$ matrix and can always be remedied by improving the faulty approximation.[26] In this regard, it is not surprising that a quadratic K matrix does not extend well beyond the s region for which it was designed.

IV. DISCUSSION

To summarize, we have used the K-matrix formalism to build proper kinematic and unitarity properties into a coupled-channel $\mathcal{S}$ matrix for the $pp(^1D_2)$ and $n\Delta^{++}(^5S_2)$ system. We have used $pp \to pp$ elastic-scattering phase-shift solutions to determine a wide variety of reasonable K matrices. For each solution, a prediction of the S-wave $n\Delta^{++}$ elastic phase was made. In all of our solutions, a diproton resonance with parameters similar to those obtained by Hoshizaki was found on the second sheet of the pp and $np\pi^+$ unitarity cuts, and on the first sheet of the $n\Delta^{++}$ cut.

Many authors[11] have been concerned that the resonancelike behavior of the $pp\,^1D_2$ wave might simply be the result of the opening of the $n\Delta^{++}$ channel—Hoshizaki's resonance[3] occurs very near the $n\Delta^{++}$ threshold. Our analysis suggests that this is not the case and that the diproton resonance is present even when $n\Delta^{++}$ kinematics are considered. In a preliminary analysis of the three-channel $pp(^1D_2)$, $n\Delta^{++}(^5S_2)$, and $\pi^+d(^3P_2)$ system, we obtain results similar to those reported here—a variety of phase-shift behaviors for the unconstrained $n\Delta^{++}$ and π^+d channels emerge and, in all cases, a diproton resonance is found. However, the uncertainties involved in reducing the problem to a small number of quasi-two-body channels must be considered and these uncertainties preclude making a definitive statement on the existence of the diproton.

Supposing the existence of the diproton resonance was unambiguously established, its theoretical interpretation would still be subject to considerable debate. Is the resonance a tightly bound six-quark object, such as the ones suggested by Jaffe,[27] or is it a molecularlike object of two spatially separated baryons such as the deuteron? While our approach should in principle shed some light on this discussion, there are not enough experimental constraints to permit definite conclusions. In the following remarks we indicate some apparent features of the diproton which are common to all our solutions and some which depend on the presently unconstrained δ_2 behavior.

From the pole's location on the second sheet of the pp and $np\pi$ cuts, the diproton is seen to be unstable in the pp and $np\pi$ systems. That the pole is on the first sheet of the $n\Delta$ cut suggests it is stable in the $n\Delta$ system—the dibaryon may be a virtual bound state of n and Δ. The dibaryon pole also appears on a distant sheet (on the first sheet of the pp cut, on the second sheet of the $np\pi$ cut, and either on the first or second sheet of the $n\Delta$ cut), so it has properties in common with Breit-Wigner resonances.[25]

The importance of the interchannel coupling in the production of the resonance is closely connected to the interpretation of the nature of the resonance. Assuming, as in our analysis, that K is chosen without poles, all the poles of T arise from zeros of

$$\det(1-CK)=(1-C_1K_{11})(1-C_2K_{22})-C_1C_2K_{12}^2\,. \tag{4.1}$$

A zero of $\det(1-CK)$ may arise in one of two ways.[18] If either $(1-C_1K_{11})$ or $(1-C_2K_{22})$ has a zero and K_{12} is not large, $\det(1-CK)$ will have a nearby zero. This is interpreted to mean that one of the individual channels has a resonance and this resonance is reflected in all channels through unitarity. The other type of zero of $\det(1-CK)$ arises from a general cancellation in (4.1), with no zero of either $(1-C_1K_{11})$ or $(1-C_2K_{22})$. Unlike the first situation where a resonance is present even when $K_{12}=0$, this case requires K_{12} to be sufficiently large for a resonance to occur. Both behaviors are observed among our solutions. Those solutions with δ_2 rising to about 50^0 and leveling off (e.g., solutions 2 and 3) exhibit a zero of $(1-C_2K_{22})$ near the zero of $\det(1-CK)$, usually on the second sheet of the $n\Delta$ cut. For these solutions the dibaryon seems to be a feature of the $n\Delta$ system which is visible in the pp channel through unitarity. Those solutions with δ_2 small and then negative (e.g., solutions 1 and 4) have no zero of $(1-C_1K_{11})$ or $(1-C_2K_{22})$—the zero of $\det(1-CK)$ arises through a general cancellation and the dibaryon is a feature of the full coupled-channel problem

It is tempting to use Levinson's theorem to identify those solutions with positive δ_2 with an unstable elementary particle or a dynamical resonance depending on whether

$$\delta_1(\infty)+\delta_2(\infty)=\pi \text{ or } 0\,,$$

respectively. Similarly, it is tempting to identify the solutions with negative δ_2 with a dynamical resonance or virtual bound state of a higher channel depending on whether

$$\delta_1(\infty)+\delta_2(\infty)=0 \text{ or } -\pi\,,$$

respectively. Implicit in this discussion is the assumption that a multichannel relativistic Levinson's theorem is meaningful[26,28] and that the asymptotic phases may be identified at these low energies. While the above classifications may not be strictly justified, we believe they provide useful mnemonics for the two types of solutions that have been found.

A serious question that can be raised at this point is will we ever be able to experimentally distinguish these two classes of solutions? The only possibility at this time is to make use of inelastic polarization data to try a crude inelastic partial-wave analysis. If this proves impractical further insight may have to depend upon theoretical models.

ACKNOWLEDGMENTS

During the course of this project we have received valuable assistance from our experimental and theoretical colleagues. We are particularly grateful to A. Yokosawa and the ANL polarized-target group for discussions concerning their data, and for providing us with access to Hoshizaki's phase-shift program. One of us (G.H.T.) wishes to thank G. C. Phillips and colleagues at the Bonner Nuclear Laboratory for stimulating discussion on final-state interactions and dibaryon resonances which initiated this work. We have alse benefited from many discussions with C. Sorensen and A. B. Wicklund on a variety of aspects of this project. Finally, it is a pleasure to acknowledge several conversations with E. L. Berger for imparting to us some of his expertise on the methodology which we have adopted, and for his critical reading of the manuscript. This work was performed under the auspices of the United States Department of Energy and was supported in part by the Natural Sciences and Engineering Research Council of Canada.

APPENDIX: THE ANALYTIC CONTINUATION OF THE CHEW-MANDELSTAM FUNCTION

Throughout this analysis the square-root function is assumed to be cut from $-\infty$ to 0. Figure 5 illustrates the cut structure of C_1 and C_2.

The definitions (2.16) and (2.17) for ρ_1 and C_1 may be used on the first sheet of the pp cut (I). On the second sheet (II),

$$C_1^{\mathrm{II}}(s,m_p,m_p)=C_1^{\mathrm{I}}(s,m_p,m_p)-2i\epsilon\rho_1^{\mathrm{I}}(s,m_p,m_p)\,, \tag{A1}$$

where $\epsilon=1$ for $\mathrm{Im}(s-4m_p^2)>0$ and $\epsilon=-1$ for $\mathrm{Im}(s-4m_p^2)<0$.

The definition (2.22) of C_2 may be used straightforwardly on the first sheet of the $np\pi^+$ cut (I); however, care must be taken when extending this definition to the second sheet of the $np\pi^+$ (II) and to the second sheet of the $n\Delta^{++}$ cut (III) because of the presence of pinching singularities in the integral (2.22). An analytic weighting function is defined as

$$W(s')=\frac{f^2[s'-(m_p+m_\pi)^2]\rho^{L=0}(s',m_p,m_\pi)}{d(s')\{d(s')-2if^2[s'-(m_p+m_\pi)^2]\rho^{L=0}(s',m_p,m_\pi)\}}\,. \tag{A2}$$

The definition (3.7) becomes

$$C_2^{\mathrm{I}}(s,m_\Delta^*,m_n)=\frac{1}{\pi}\int_{(m_p+m_\pi)^2}^{\infty}ds'\,W(s')C_2^{\mathrm{I}}(s,\sqrt{s'},m_n)\,, \tag{A3}$$

where $C_2^{\mathrm{I}}(s,\sqrt{s'},m_n)$ is the naive extension of (2.19). Since this is cut from $s=(\sqrt{s'}+m_n)^2$ to infinity, $C_2^{\mathrm{II}}(s,m_\Delta^*,m_n)$ and $C_2^{\mathrm{III}}(s,m_\Delta^*,m_n)$ are built from both $C_2^{\mathrm{I}}(s,\sqrt{s'},m_n)$ and $C_2^{\mathrm{II}}(s,\sqrt{s'},m_n)$. Analogous to (A1),

$$C_2^{\mathrm{II}}(s,\sqrt{s'},m_n)=C_2^{\mathrm{I}}(s,\sqrt{s'},m_n)-2i\epsilon\rho_2^{\mathrm{I}}(s,\sqrt{s'},m_n)\,, \tag{A4}$$

where $\epsilon=1$ for $\mathrm{Im}[s-(\sqrt{s'}+m)^2]>0$ and $\epsilon=-1$ for $\mathrm{Im}[s-\sqrt{s'}+m)^2]<0$. The smeared $n\Delta^{++}$ Chew-Mandelstam function on the second sheet of the $np\pi^+$ cut is

$$\begin{aligned}C_2^{\mathrm{II}}(s,m_\Delta^*,m_n)=&\frac{1}{\pi}\int_{(m_p+m_\pi)^2}^{\mathrm{Re}[(\sqrt{s}-m_n)^2]}ds'\,W(s')C_2^{\mathrm{II}}(s,\sqrt{s'},m_n)+\frac{1}{\pi}\int_{\mathrm{Re}[(\sqrt{s}-m_n)^2]}^{(\sqrt{s}-m_n)^2}ds'\,W(s')[C_2^{\mathrm{II}}(s,\sqrt{s'},m_n)-C_2^{\mathrm{I}}(s,\sqrt{s'},m_n)]\\&+\frac{1}{\pi}\int_{\mathrm{Re}[(\sqrt{s}-m_n)^2]}^{\infty}ds'\,W(s')C_2^{\mathrm{I}}(s,\sqrt{s'},m_n)\,.\end{aligned} \tag{A5}$$

Using (A4),

$$C_2^{\mathrm{II}}(s,m_\Delta^*,m_n)=C_2^{\mathrm{I}}(s,m_\Delta^*,m_n)-\frac{2i\epsilon}{\pi}\int_{(m_p+m_\pi)^2}^{(\sqrt{s}-m_n)^2}ds'\,W(s')\rho_2^{\mathrm{I}}(s,\sqrt{s'},m_n)\,. \tag{A6}$$

The $n\Delta^{++}$ cut now appears through the integral in (A6) and may be exhibited explicitly by performing the integration over the pole piece of $W(s')$. We are interested in the part of sheets II and III nearest the physical region, i.e., $\mathrm{Im}s<0$ and so consider only the pole of $W(s')$ at $s'=(m_\Delta^*)^2$. We define

$$\tilde{W}(s')=\frac{1}{-2id'(m_\Delta^{*2})}\frac{1}{s'-m_\Delta^{*2}}\,. \tag{A7}$$

There is also a pole at $s'=(\overline{m_\Delta^*})^2$ which would affect the evaluation of (A6) for $\mathrm{Im}(s)>0$. Specializing to $\mathrm{Im}s<0$,

$$C_2^{\rm II}(s,m_\Delta^*,m_n)=C_2^{\rm I}(s,m_\Delta^*,m_n)+\frac{2i}{\pi}\int_{(m_p+m_\pi)^2}^{(\sqrt{s}-m_n)^2}ds'[W(s')-\tilde{W}(s')]\rho_2^{\rm I}(s,\sqrt{s'},m_n)$$

$$-\frac{1}{\pi d'(m^{*2})}\int_{(m_p+m_\pi)^2}^{(\sqrt{s}-m_n)^2}ds'\,\frac{1}{s'-m_\Delta^{*2}}\,\rho_2^{\rm I}(s,\sqrt{s'},m_n)\,. \tag{A8}$$

The $n\Delta^{++}$ cut appears only in the last integral and the first two terms are numerically stable in the vicinity of this cut. The last integral becomes

$$\int_{(m_p+m_\pi)^2}^{(\sqrt{s}-m_n)^2}ds'\,\frac{1}{s'-m_\Delta^{*2}}\,\rho_2^{\rm I}(s,\sqrt{s'},m_n)$$

$$=\frac{1}{s}\Bigg\{-[(\sqrt{s}-m_n)^2-(m_p+m_\pi)^2]^{1/2}[(\sqrt{s}+m_n)^2-(m_p+m_\pi)^2]^{1/2}$$

$$-2(s+m_n^{\,2}-m_\Delta^{*2})\ln\frac{[(\sqrt{s}-m_n)^2-(m_p+m_\pi)^2]^{1/2}+[(\sqrt{s}+m_n)^2-(m_p+m_\pi)^2]^{1/2}}{2(\sqrt{s}m_n)^{1/2}}$$

$$+2[(\sqrt{s}-m_n)^2-m_\Delta^{*2}]^{1/2}[(\sqrt{s}+m_n)^2-m_\Delta^{*2}]^{1/2}$$

$$\times\Bigg[\ln\frac{[(\sqrt{s}+m_n)^2-m_\Delta^{*2}]^{1/2}[(\sqrt{s}-m_n)^2-(m_p+m_\pi)^2]^{1/2}+[(\sqrt{s}-m_n)^2-m_\Delta^{*2}]^{1/2}[(\sqrt{s}+m_n)^2-(m_p+m_\pi)^2]^{1/2}}{[m_\Delta^{*2}-(m_p+m_\pi)^2]^{1/2}[4\sqrt{s}m_n]^{1/2}}$$

$$-i\epsilon\pi/2\Bigg]\Bigg\}\,, \tag{A9}$$

where

$\epsilon=1$ for $\mathrm{Im}[(\sqrt{s}-m_n)^2-m_\Delta^{*2}]>0$

and

$\epsilon=-1$ for $\mathrm{Im}[(\sqrt{s}-m_n)^2-m_\Delta^{*2}]<0$.

On the second sheet of the $n\Delta^{++}$ cut (III), $C_2^{\rm III}$ has the same form as $C_2^{\rm II}$, (A8) and (A9), with just the sign of ϵ reversed.

[1]The experimental situation is reviewed by A. Yokosawa, Argonne Report No. ANL-HEP-PR-80-16 (unpublished).

[2]K. Hidaka, A. Beretvas, K. Nield, H. Spinka, D. Underwood, Y. Watanabe, and A. Yokosawa, Phys. Lett. 70B, 479 (1977), and references therein.

[3]N. Hoshizaki, Prog. Theor. Phys. 60, 1796 (1978); 61, 129 (1979).

[4]R. A. Arndt, talk given during LAMPF Nucleon-Nucleon Workshop, 1978 (unpublished); these phase shifts were made available to us by A. Yokosawa.

[5]D. V. Bugg, Nucl. Phys. G5, 1349 (1979); C. L. Hollas, Phys. Rev. Lett. 44, 1186 (1980).

[6]J. S. Ball and W. R. Frazer, Phys. Rev. Lett. 7, 204 (1961); J. S. Ball, W. R. Frazer, and M. Nauenberg, Phys. Rev. 128, 478 (1962).

[7]R. S. Longacre, T. Lasinski, A. H. Rosenfeld, G. Smadja, R. J. Cashmore, and D. W. G. S. Leith, Phys. Rev. D 17, 1795 (1978).

[8]See, for example, R. E. Cutkosky, H. R. Hicks, J. Sandusky, C. C. Shin, R. L. Kelly, R. C. Miller, and A. Yokosawa, Nucl. Phys. B102, 139 (1976); R. L. Kelly, in *High Energy Physics with Polarized Beams and Polarized Targets*, proceedings of the Third International Symposium, Argonne, Illinois, edited by G. H. Thomas (AIP, New York, 1979), p. 501; R. A. Arndt, L. D. Roper, and P. H. Steinberg, Phys. Rev. D 18, 3278 (1978).

[9]J. L. Basdevant and E. L. Berger, Phys. Rev. Lett. 37, 977 (1976); Phys. Rev. D 16, 657 (1977); Phys. Rev. Lett. 40, 994 (1978); Phys. Rev. D 19, 246 (1979).

[10]J. L. Basdevant and E. L. Berger, Phys. Rev. D 19, 239 (1979).

[11]R. A. Arndt, Phys. Rev. 165, 1834 (1968); G. L. Kane and G. H. Thomas, Phys. Rev. D 13, 2944 (1976); L. M. Libby and E. Predazzi, Lett. Nuovo Cimento, Vol. II, N18, 881 (1969); J. H. Hall, T. A. Murray, and L. Riddiford, Nucl. Phys. B12, 573 (1969); H. Suzuki, Prog. Theor. Phys. 54, 143 (1975); D. D. Brayshaw, Phys. Rev. Lett. 37, 1329 (1976); B. J. Edwards and A. N. Kamal, Can. J. Phys. 57, 659 (1979). Additional references may be found in G. H. Thomas, in *Few Body Systems and Nuclear Forces II*, proceedings of the VIII International Conference, Graz, Austria, 1978, edited by H. Zingl, M. Haftel, and H. Zankel (Springer, Berlin, 1978), p. 86; N. Hoshizaki, talk presented at the 1979 INS Symposium on Particle Physics in GeV Region, Tokyo, 1979 (unpublished).

[12]E. L. Berger, P. Pirilä, and G. H. Thomas, Report No. ANL-HEP-PR-75-72 (unpublished).

[13]S. Mandelstam, Proc. Phys. Soc. London, Sect. A244, 491 (1958).

[14]D. V. Bugg, Nucl. Phys. G5, 1349 (1977).

[15]P. Walden, D. Ottewell, E. L. Mathie, T. Masterson,

G. Jones, R. R. Johnson, A. Haynes, and E. G. Auld, Phys. Lett. 81B, 156 (1979).
[16]This importance of considering three channels was pointed out to us by E. Berger (private communication).
[17]R. H. Dalitz, *Strange Particles and Strong Interactions* (Oxford University Press, London, 1962).
[18]R. Levi Setti and T. Lasinski, *Strongly Interacting Particles* (University of Chicago Press, Chicago, 1973).
[19]Our formalism parallels that given in Refs. 9 and 10.
[20]N. I. Muskhelishvili, *Singular Integral Equations* (Noordhoff, Groningen, 1953); R. Omnès, Nuovo Cimento 8, 316 (1958); O. Babelon, J. L. Basdevant, D. Caillerie, and G. Mennessier, Nucl. Phys. B113 445 (1976).
[21]J. R. Carter, D. V. Bugg, and A. A. Carter, Nucl. Phys. B58, 378 (1973); G. Rowe, M. Salomon, and R. H. Landau, Phys. Rev. C 18, 584 (1978).
[22]Particle Data Group, Phys. Lett. 75B, 1 (1978).
[23]A. B. Wicklund (private communication); M. Arenton, D. Ayres, R. Diebold, E. May, L. Nodulman, J. Sauer, A. B. Wicklund, and E. Swallow, Argonne report, 1979 (unpublished).
[24]J. S. Ball, P. S. Lee, and G. L. Shaw, Phys. Rev. D 7, 2789 (1973).
[25]D. Morgan, Phys. Lett. 51B, 71 (1974).
[26]S. C. Frautschi, *Regge Poles and S-Matrix Theory* (Benjamin, New York, 1963).
[27]R. J. Jaffe, Phys. Rev. Lett. 38, 195 (1977); 38, 617 (1977). See also P. J. G. Mulders, A. Th. M. Aerts, and J. J. de Swart, Phys. Rev. Lett. 40, 1543 (1978).
[28]M. Kato, Ann. Phys. (N.Y.) 31, 130 (1965).